Mesoporous Materials

DOI: 10.1002/anie.201305527

A Shear Stress Regulated Assembly Route to Silica Nanotubes and Their Closely Packed Hollow Mesostructures**

Chun Wang, Jing Wei, Qin Yue, Wei Luo, Yuhui Li, Minghong Wang, Yonghui Deng, and Dongyuan Zhao*

Self-assembly of amphiphilic molecules has enabled the fabrication of abundant nanostructured materials for different applications.[1] Since the discovery of M41S family ordered mesoporous silicates,[2] numerous ordered mesoporous materials have been synthesized.[3–5] Huo et al.[6] have intensively investigated structure-directing roles of various quaternary ammonium surfactants, and phase transition between different silica-based mesophases. To date, different mechanisms for the formation of mesostructures have been proposed, like true liquid-crystal templating (LCT)[7] and cooperative self-assembly (CSA),[8] wherein the surfactant micelles are encapsulated in the frameworks of the other components as the consolidated phases. Particularly, Davis and co-workers have firstly suggested a "silicate rod assembly" route, where randomly ordered surfactant/silicate composite nanorods can spontaneously pack into a long-range ordered hexagonal arrangement.[9] This mechanism, although it provides an explicit picture of the whole assembly process, still calls for more convincing evidences.

Since small-molecule surfactants and commercial Pluronic triblock copolymers can only yield mesoporous materials with pore sizes below 12 nm without adding pore-expanding agents, the demand of ordered mesoporous materials with large pores has attracted considerable interest. After the first report by Templin et al.,[10] diblock copolymers have become attractive alternatives in the soft-templating syntheses of ordered mesoporous materials, especially those with large pores.[11–14] Previous work has mainly focused on the core/shell-type nanostructured materials based on single spherical micelles or just their aggregated counterparts. However, till now, seldom work on the cooperative self-assembly of diblock copolymers with the corresponding inorganic species into tubular mesostructures and systematic structure-directing roles of diblock copolymers in the formation of mesostructures was reported.

Herein, we report an assembly route that is regulated by shear stress to fabricate uniform silica nanotubes and their closely packed hollow mesostructures. The as-made silica/template composites can be spontaneously packed into ordered hexagonal mesostructures (*p6mm*) with uniform large bimodal mesopores. We attribute the formation of this quasi-stable mesostructure to synergistic effects between the speeds of assembly of the preformed spherical micelles as the building mesoblocks, and hydrolysis and condensation of the silica precursors. Uniform gold nanoparticles were introduced onto the surface of the interior cavities of the ethenyl-modified silica nanotubes (E-SNTs). The Au/E-SNT catalysts showed superior performance in catalyzing the epoxidation of styrene with high conversion and selectivity towards styrene oxide. As THF evaporates, the reaction mixture experiences a subtle transition from a clear transparent to a slightly blue colloid solution, to a sky-blue colloid mixture, to a milky white dispersion, and finally to a suspension with white precipitate. Field emission scanning electron microscopy (FESEM; Figure S1 in the Supporting Information) and TEM (Figure 1 a,b) images reveal that the as-made silica/template composites have a typical 1-D rod-like morphology with hemisphere-like tips. HRTEM and FESEM (Figure 1 c–f) images exhibit that the silica nanotubes retained the typical 1-D mesostructure. Although the randomly distributed bundle is the predominant structural type observed in the HRTEM images owing to the sintering effect by calcination, some separated silica nanotubes are still visible in most areas. The obtained silica nanotubes have a uniform diameter of 40–50 nm and length of 400–500 nm. The silica nanotubes possess undulating surfaces and channels with occasionally several adhered spherical micelles (Figure 1 b), suggesting that spherical micelles might be the building units. N_2 isotherms show representative type IV curves with a sharp capillary condensation step in the relative pressure range of 0.92–0.98 (Figure S2A in the Supporting Information). Pore-size distributions (Figure S2B) reveal mesopores of 2.0, 5.5, and 40 nm, which are derived from nanopores in the defects of silica walls, voids among the bundles of the silica tubes, and the tubular mesopores, respectively. Control experiments under static but otherwise identical conditions yielded ordered (cubic close packed, *fcc*) mesoporous silicas with large pores (Figures S3, S4 in the Supporting Information), similar to our previous report.[14a]

[*] C. Wang, J. Wei, Q. Yue, W. Luo, Y. H. Li, M. H. Wang, Prof. Dr. Y. H. Deng, Prof. Dr. D. Y. Zhao
Department of Chemistry, Laboratory of Advanced Materials
Shanghai Key Lab of Molecular Catalysis and Innovative Materials
and State Key Laboratory of Molecular Engineering of Polymers
Fudan University
Shanghai 200433 (P. R. China)
E-mail: yhdeng@fudan.edu.cn

[**] This work was supported by the State Key 973 Program of PRC (2013CB934104 and 2012CB224805), the NSF of China (21073040, 51372041 and 21210004), the specialized research fund for the doctoral program of higher education of China (20120071110007), the innovation program of Shanghai Municipal Education Commission (13ZZ004), Shanghai Rising Star Project of STCSM (12QH1400300), and the Program for New Century Excellent Talents in University (NCET-12-0123).

Supporting information for this article is available on the WWW under http://dx.doi.org/10.1002/anie.201305527.

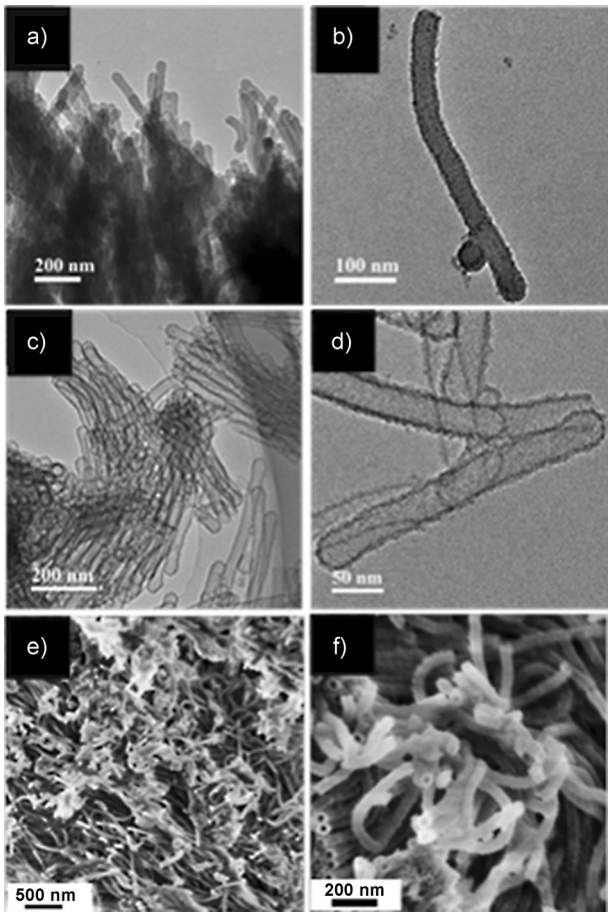

Figure 1. TEM images (a, b) of the as-made silica/template composites templated by the diblock copolymer poly(ethylene oxide)-*b*-polystyrene (PEO-*b*-PS) under mild stirring by using the shear stress regulated assembly route. HRTEM (c, d) and FESEM (e, f) images of the silica nanotubes obtained after a hydrothermal treatment at 100 °C for 24 h and subsequent calcination at 550 °C in air for 5 h.

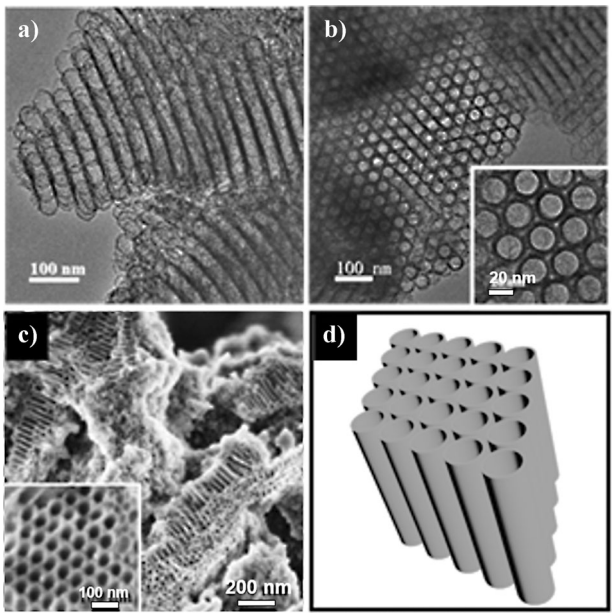

Figure 2. HRTEM (a, b) and FESEM (c) images of the ethenyl-modified organosilica nanotubes obtained after hydrothermal treatment at 100 °C for 24 h and calcination at 550 °C in air for 5 h. The insets of (b) and (c) are the corresponding magnified images. d) Corresponding illustration of 3-D structures.

HRTEM and FESEM (Figure S5a, c in the Supporting Information) images show that the carbon nanotubes obtained after direct carbonization have a well replicated 1-D structure of the as-made silica/template composites with a diameter of 40–50 nm and length of 300–500 nm. Pretreatment with sulfuric acid and further carbonization converts the diblock copolymers into carbonaceous materials. Because the amount is not sufficient to fill the entire internal hollow channels, the carbonaceous materials prefer to deposit on the internal surface owing to the high surface energy of the pore walls, similar to the example reported before.[15] After removal of silica, the 1-D mesostructure of the as-made silica/template composites can be well preserved without obvious structural collapse. The undulating surface of the carbon nanotubes can also be observed from FESEM images (Figure S5c), suggesting that the as-made silica/template composites effectively function as the templates.

HRTEM and FESEM images (Figure 2 a–c) of the ethenyl-modified organosilica nanotubes show tubes with a diameter of approximately 50 nm and length of approximately 200 nm, which are assembled into hexagonal ordered mesostructures (*p6mm*) within a rather large domain; these structures are seemly similar to that of SBA-15 templated by Pluronic P123. Particularly, two types of pores could be clearly indentified (i.e. cylindrical pores from the interior voids of the silica nanotubes and packing cavities between ordered packed nanotubes), indicating that the current mesostructure is related with packing of nanotubes. A well-resolved scattering peak can be observed in the SAXS patterns (Figure S6 in the Supporting Information), suggesting a hexagonal ordered mesostructure. Typical type IV isotherm curves and a distinct bimodal pore size distribution (20 and 34 nm) can be clearly indentified (Figure S7 in the Supporting Information), which is very different from that for SBA-15.

All these results suggest that stirring is a crucial parameter for the formation of these rod-shaped nanocomposites. As a representative example of a 1-D nanomaterial, silica nanotubes belong to the most favorable nanostructures because of their remarkable physicochemical properties and potential applications.[16–18] Previously, silica nanotubes were mostly synthesized by using different templates.[19–23] To our knowledge, this is the first report on the synthesis of uniform silica nanotubes from diblock copolymers by using a mild sol–gel process. Compared to the hard-templating method, the soft-templating synthesis based on the interaction and self-assembly of silica precursors with diblock copolymers undergoes in a subtler way, which is similar to the ubiquitous biosilification process in biosynthesis, and can improve our understanding of the laws of the sophisticated molecular tectonics in nature.

Based on the above results, we attribute the formation of the mesoporous silica nanotubes and their closely packed

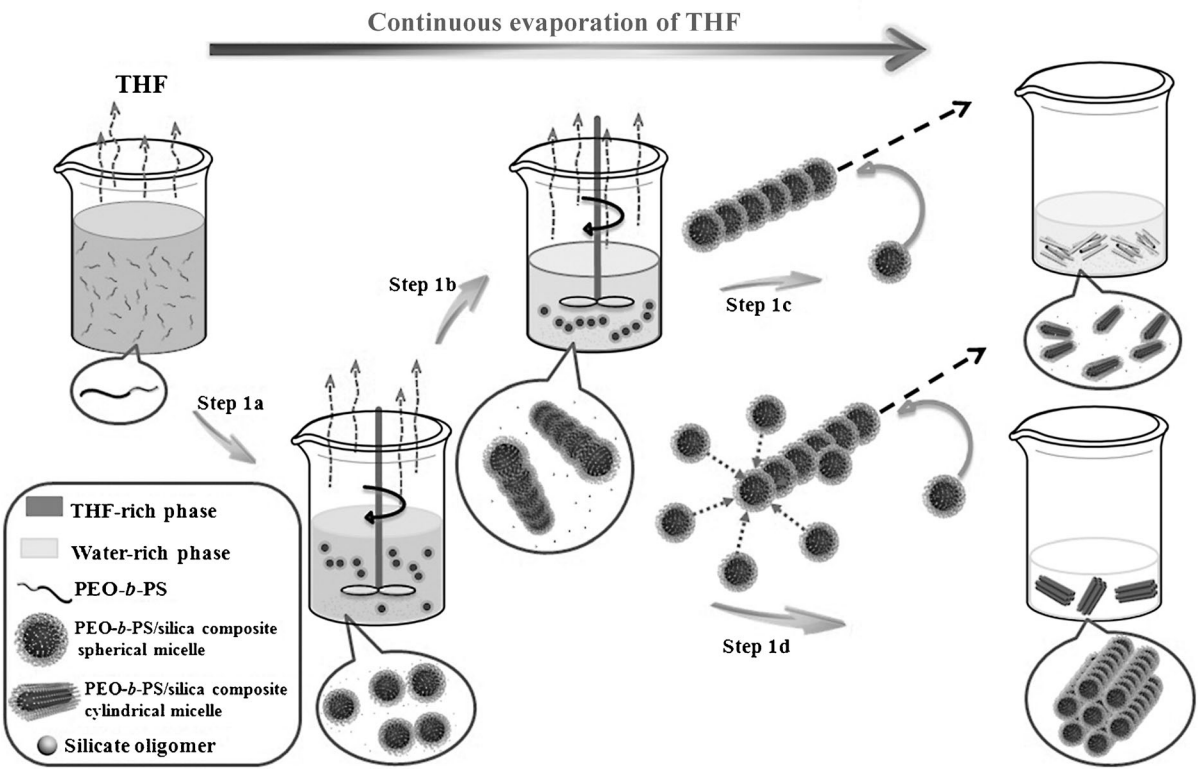

Scheme 1. The formation mechanism of the mesoporous silica nanotubes and their closely packed hollow mesostructures through the shear stress regulated assembly route. Step 1a: formation of PEO-*b*-PS/silica spherical micelles, serving as the *meso*-building blocks for the further assembly. Step 1b: formation of the rod-like micelles for the decrease in the curvature of the micelles under the shear stress derived from stirring. As THF further evaporates, the preformed spherical micelles tend to aggregate through head-to-head packing into spheroidal mesostructures owing to the cross-linking and polymerization of the silicates on the shell surface, thereby forming 1-D calabash-like mesostructured rods along the *c*-axial direction (the long-axial direction of the hexagonal mesostructure). Step 1c: the rod-shaped micelles aggregate together into bundles driven by the strong hydrogen bonding. As more PEO-*b*-PS/silica composite rods form and THF evaporates, the cross-linking and polymerization of silicates can be accelerated by hydrochloric acid catalysis, forming PEO-*b*-PS/silica composite bundles. Step 1d: the formation of hexagonal hollow mesostructures as a result of the coexistence of dominated head-to-head assembly of the preformed spherical micelles along the normal direction (*c*-axial) and further accelerated hydrolysis and condensation of the silicate precursors in the tangential direction (*a*-axial direction of hexagonal mesostructure) of the stirring leading to side-to-side attachment of spherical micelles in a hexagonal pattern.

hollow mesostructures to a shear stress regulated assembly route (Scheme 1, Figure S9 in the Supporting Information). As THF evaporates, amphiphilic diblock copolymer containing hydrophilic PEO and hydrophobic PS block can readily self-assemble into spherical micelles with PS as the core surrounded by a PEO shell. After introduction of the silica precursor, silicate oligomers can associate with PEO moieties through hydrogen bonding through hydrochloric acid, thereby forming PEO-*b*-PS/silica spherical micelles as a *meso*-building block. If mild stirring is adopted, the hydrolysis and condensation of silica precursors in the tangential direction of the stirring are depressed to some extent, and thus head-to-head assembly of the preformed spherical micelles along the normal direction dominates (step 1a). As the rod-like micelles elongate, the mesostructure of the nanocomposites experiences a subtle transition from spherical, to spheroidal, to final tubular micelles (step 1b). Owing to the inadequate polymerization of silica precursors, many nodes and round ends of the nanotubes can be clearly identified. As a large number of siloxanes (Si-O-Si) exist on the surface, the micelles aggregate together into bundles driven by strong hydrogen bonding (step 1c). The introduction of organosilane, however, hydrolysis and condensation of the silica precursor are accelerated. Hexagonal hollow mesostructures are formed (step 1d) owing to the coexistence of the dominating head-to-head assembly of the preformed spherical micelles along the normal direction (*c*-axial, the long-axial direction of the hexagonal structure) of the stirring and the accelerated hydrolysis and condensation of silica precursors in the tangential direction (*a*-axial direction of the hexagonal structure) of the stirring, thereby leading to side-to-side attachment of spherical micelles in a hexagonal pattern.

The hollow mesostructures with highly accessible bimodal pores are appropriate for loading functional nanoparticles for catalysis. HRTEM images (Figure 3 a,b) revealed that the parent E-SNTs, as a host, retained the typical 1-D mesostructure after loading with Au nanoparticles. The encapsulated uniform Au nanoparticles are homogeneously confined in the hollow channels of the ordered packed nanotubes. Furthermore, Au nanoparticles with lattice fringes spacing (Figure 3 c) of approximately 0.23 nm, corresponding to the (111) planes of the gold nanocrystals, can be clearly identified. XRD pattern (Figure S8 in the Supporting Information)

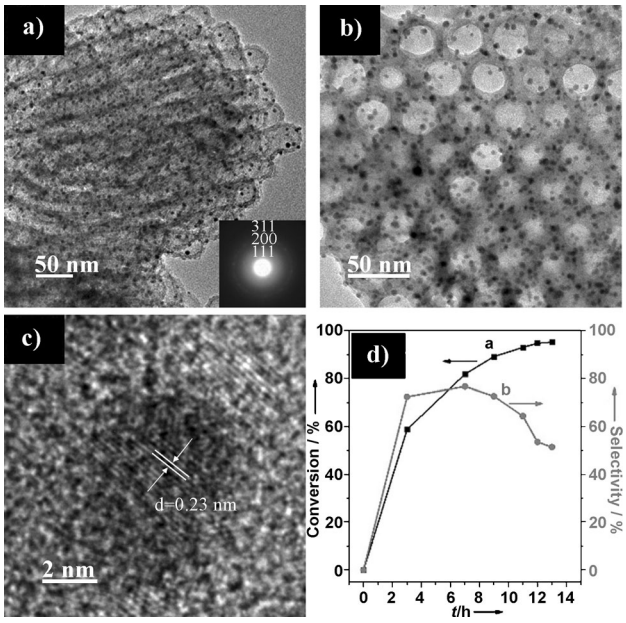

Figure 3. HRTEM images (a, b) of the Au/E-SNT composites. Inset of (a) is the corresponding selected-area electron diffraction (SAED) pattern, confirming that the Au nanoparticles have an *fcc* structure. c) HRTEM image of the Au nanoparticles. d) The conversion of styrene (curve a) and selectivity of the conversion to styrene oxide (curve b) as a function of reaction time.

shows typical wide diffraction peaks, which can be assigned to Au nanoparticles with an *fcc* structure. The conversion of styrene increases promptly and reaches almost 95.3% at 13 h (Figure 3d), thus suggesting that Au/E-SNTs have a rather high catalytic activity. The selectivity of the reaction to give styrene oxide reaches about 76.8% after 7 h and then decreases slightly, which is mainly caused by the isomerization of styrene oxide or overoxidation at high temperature. Considering both conversion and selectivity, it can be concluded that the present catalyst can achieve high conversion (81.9%) and selectivity (76.8%) just after reaction for 7 h, which is higher[14b,24] than that reported. The remarkable catalytic performance might stem from the well-confined Au nanoparticles, their thermally and chemically stable silica-based frameworks, and particularly, the highly accessible bimodal channel-like pore mesostructure favoring enhanced diffusion.

In summary, a shear stress regulated assembly route to fabricate silica nanotubes and their closely packed hollow mesostructures was reported. The as-made silica/template composites can be packed into ordered mesostructures with bimodal mesopores. Uniform gold nanoparticles were encapsulated onto the surface of the interior cavities of the ethenyl-modified silica nanotubes. The Au/E-SNT catalysts exhibited superior performance in catalyzing epoxidation of styrene with high conversion and selectivity towards styrene oxide. We believe that this shear stress regulated assembly route can be extended to other soft-templating synthesis systems for rationally tailoring the micelle particle growth patterns, which are not only of academic interests, but also can lead to construction of more nanomaterials in the near future.

Received: June 27, 2013
Revised: July 26, 2013
Published online: September 5, 2013

Keywords: block copolymers · mesoporous materials · nanotubes · shear stress

[1] a) Y. Y. Mai, A. Eisenberg, *Chem. Soc. Rev.* **2012**, *41*, 5969; b) C. Fong, T. Le, C. J. Drummond, *Chem. Soc. Rev.* **2012**, *41*, 1297.
[2] C. T. Kresge, M. E. Leonowicz, W. J. Roth, J. C. Vartuli, J. S. Beck, *Nature* **1992**, *359*, 710.
[3] S. A. Bagshaw, E. Prouzet, T. J. Pinnavaia, *Science* **1995**, *269*, 1242.
[4] D. Y. Zhao, J. L. Feng, Q. S. Huo, N. Melosh, G. H. Fredrickson, B. F. Chmelka, G. D. Stucky, *Science* **1998**, *279*, 548.
[5] a) Y. Wan, D. Y. Zhao, *Chem. Rev.* **2007**, *107*, 2821; b) Y. H. Deng, J. Wei, Z. K. Sun, D. Y. Zhao, *Chem. Soc. Rev.* **2013**, *42*, 4054.
[6] Q. S. Huo, D. I. Margolese, G. D. Stucky, *Chem. Mater.* **1996**, *8*, 1147.
[7] G. S. Attard, J. C. Glyde, C. G. Goltner, *Nature* **1995**, *378*, 366.
[8] A. Monnier, F. Schuth, Q. Huo, D. Kumar, D. Margolese, R. S. Maxwell, G. D. Stucky, M. Krishnamurty, P. Petroff, A. Firouzi, M. Janicke, B. F. Chmelka, *Science* **1993**, *261*, 1299.
[9] C. Y. Chen, S. Q. Xiao, M. E. Davis, *Microporous Mater.* **1995**, *4*, 1.
[10] M. Templin, A. Franck, A. D. Chesne, H. Leist, Y. M. Zhang, R. Ulrich, V. Schädler, U. Wiesner, *Science* **1997**, *278*, 1795.
[11] J. Lee, M. C. Orilall, S. C. Warren, M. Kamperman, F. J. Disalvo, U. Wiesner, *Nat. Mater.* **2008**, *7*, 222.
[12] K. Yu, A. J. Hurd, A. Eisenberg, C. J. Brinker, *Langmuir* **2001**, *17*, 7961.
[13] Q. Yue, M. H. Wang, J. Wei, Y. H. Deng, T. Y. Liu, R. C. Che, B. Tu, D. Y. Zhao, *Angew. Chem.* **2012**, *124*, 10514; *Angew. Chem. Int. Ed.* **2012**, *51*, 10368.
[14] a) J. Wei, H. Wang, Y. H. Deng, Z. K. Sun, L. Shi, B. Tu, M. Luqman, D. Y. Zhao, *J. Am. Chem. Soc.* **2011**, *133*, 20369; b) J. Wei, Q. Yue, Z. K. Sun, Y. H. Deng, D. Y. Zhao, *Angew. Chem.* **2012**, *124*, 6253; *Angew. Chem. Int. Ed.* **2012**, *51*, 6149; c) J. Wei, Y. H. Li, M. H. Wang, Q. Yue, Z. K. Sun, C. Wang, Y. J. Zhao, Y. H. Deng, D. Y. Zhao, *J. Mater. Chem. A* **2013**, *1*, 8819–8827.
[15] J. Kim, J. Lee, T. Hyeon, *Carbon* **2004**, *42*, 2711.
[16] X. F. Yang, H. Tang, K. S. Cao, H. J. Song, W. C. Sheng, Q. Wu, *J. Mater. Chem.* **2011**, *21*, 6122.
[17] H. J. Chang, Y. F. Chen, H. P. Lin, C. Y. Mou, *Appl. Phys. Lett.* **2001**, *78*, 3791.
[18] M. Zhang, E. Ciocan, Y. Bando, K. Wada, L. L. Cheng, P. Pirouz, *Appl. Phys. Lett.* **2002**, *80*, 491.
[19] B. C. Satishkumar, A. Govindaraj, E. M. Vogl, L. Basumallick, C. N. R. Rao, *J. Mater. Res.* **1997**, *12*, 604.
[20] C. R. Martin, *Science* **1994**, *266*, 1961.
[21] M. Müllner, T. Lunkenbein, J. Breu, F. Caruso, A. H. E. Müller, *Chem. Mater.* **2012**, *24*, 1802.
[22] M. Harada, M. Adachi, *Adv. Mater.* **2000**, *12*, 839.
[23] M. Mandal, M. Kruk, *Chem. Mater.* **2012**, *24*, 123.
[24] a) S. B. Kumar, S. P. Mirajkar, G. C. G. Pais, P. Kumar, R. Kumar, *J. Catal.* **1995**, *156*, 163; b) R. Xu, D. S. Wang, J. Y. Zhang, Y. D. Li, *Chem. Asian J.* **2006**, *1*, 888.

